Energy Transfer in Bichromophoric Molecules: The Effect of Symmetry and Donor/Acceptor Energy Gap

W. T. Yip[†] and Donald H. Levy*

Department of Chemistry and James Franck Institute, University of Chicago, Chicago, Illinois 60637

Renata Kobetic and Piotr Piotrowiak*

Department of Chemistry, Rutgers University, Newark, New Jersey 07102

Received: July 22, 1998; In Final Form: November 3, 1998

The dependence of the rate of singlet excitation transfer on the donor−acceptor energy gap was investigated in bichromophoric spiranes with symmetry-forbidden zero-order electronic coupling. The fluorescence measurements were performed in a supersonic jet in order to avoid collisional and inhomogeneous line broadening. Fluorescence excitation spectra and single-vibronic-level emission spectra of the model chromophores cyclopentaphenanthrene and 1,8-dimethylnaphthalene and the bichromophores spirofluorenephenanthrene and spirofluorenenaphthalene are presented and analyzed. Although the transition moments of the linked chromophores are rigorously perpendicular and the exchange coupling between the $v' = 0$ states is computationally shown to be zero, all spiranes with energy gaps larger than ~1000 cm^{-1} exhibited complete electronic energy transfer from all vibrational states of the electronically excited donor, including the undistorted $v' = 0$ state. This behavior is explained in terms of vibronic coupling between the sparse states of the donor and the dense manifold (pseudocontinuum) of the acceptor states. The electronic energy transfer was sufficiently fast to result in measurable lifetime broadening of the donor absorption lines, from which the k_{EET} was estimated. The results demonstrate that the zero-order picture overestimates the degree of the molecular orbital symmetry control over electronic energy transfer and charge-transfer rates and that at sufficiently high driving forces the vibronically mediated "symmetry-forbidden" electronic energy transfer can be very rapid ($\sim 1 \times 10^{12}$ s^{-1}).

Introduction

The rate of electronic excitation transfer and charge-transfer processes in linked donor−acceptor systems and in bichromophoric molecules is determined by the electronic coupling between donor and acceptor. The symmetry of the zero-order localized molecular orbitals of the donor and the acceptor is an important factor determining the magnitude of this coupling. As a result, the mutual orientation of the donor and the acceptor moieties and the symmetry of the relevant molecular orbitals are frequently invoked when a particularly low or high transfer rate is observed. While the general orientational and stereochemical effects in electronic energy transfer (both dipole−dipole and exchange coupled) and charge transfer (exchange coupled) have been studied by several groups,[1] detailed experimental investigations of systems in which the electronic coupling is completely canceled by symmetry remain very rare.[2]

In recent years, we have initiated a molecular beam fluorescence study of a series of specially designed spirobifluorenes (Figure 1a) in order to demonstrate that a total symmetry cancellation of electronic coupling (both the Coulomb and the exchange couplings) between rigidly linked orthogonal chromophores can indeed be achieved.[3] It was shown that singlet energy transfer in these systems is effectively blocked,[4] despite the close proximity of the donor and acceptor units, which are separated only by a single sp^3-hybridized carbon atom. However, these strong molecular orbital symmetry effects were observed only in nearly degenerate bichromophores (i.e., when the donor−acceptor energy gap is comparable with the spacing of the low-frequency vibrational levels) at the bottom of the respective vibrational manifolds (Figure 2a). When a sufficient amount of excess vibrational energy (typically >200 cm^{-1}) was deposited in the S_1 electronic state of the donor, singlet energy transfer due to vibronic (Herzberg−Teller) coupling occurred and was manifested by dual emission at the characteristic donor and acceptor frequencies. It was concluded that two conditions have to be satisfied in order for such zero-order, symmetry-forbidden electronic energy transfer to become weakly allowed. First, the overall symmetry of the donor−acceptor system has to be broken. Second, a vibronic level of the acceptor nearly degenerate with the appropriate level of the donor must be available.

The second of the above requirements leads directly to the topic of the present contribution. We investigate the influence of the size of the energy gap between the $v' = 0$ levels of the donor and the acceptor on the rate of singlet energy transfer in systems where the symmetry of the zero-order molecular orbital inhibits electronic interaction. To address this issue, several newly synthesized spiranes with large energy gaps approaching 4000 cm^{-1} (Figure 1b) were studied. The members of the new family of model compounds (Figure 3) (except for spirofluorenenaphthalene) have the same essential electronic symmetry as the low energy gap compounds shown in Figure 1a. The localized $S_0 \leftrightarrow S_1$ transition dipoles of the chromophores are

[†] Present address: Department of Chemistry, University of Minnesota, Minneapolis, MN 55455.

10.1021/jp9831280 CCC: $18.00
Published on Web 12/17/1998

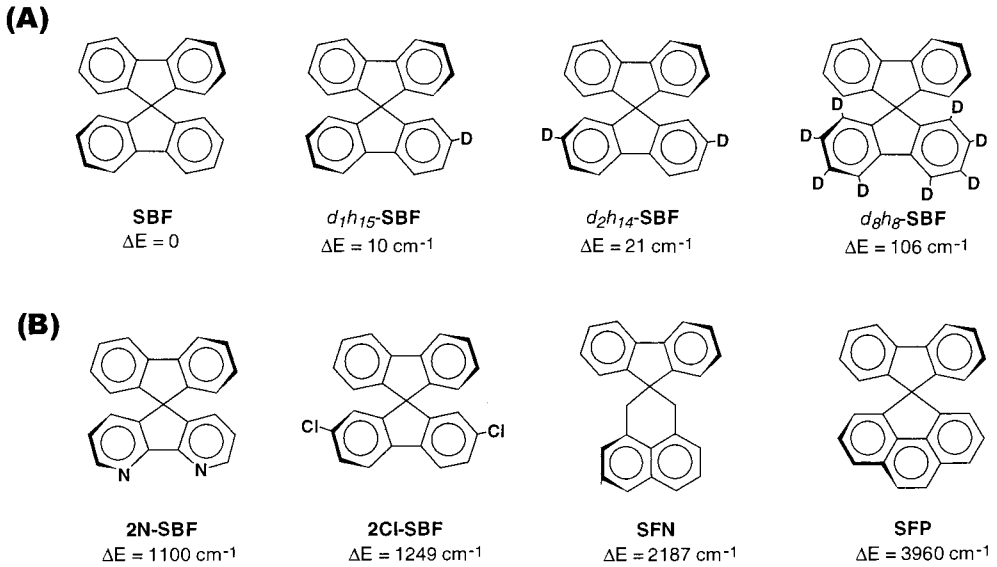

Figure 1. Spiranes with orthogonal chromophores and $S_0 \leftrightarrow S_1$ transition moments: (a) compounds with a small energy gap; (b) compounds with a large energy gap.

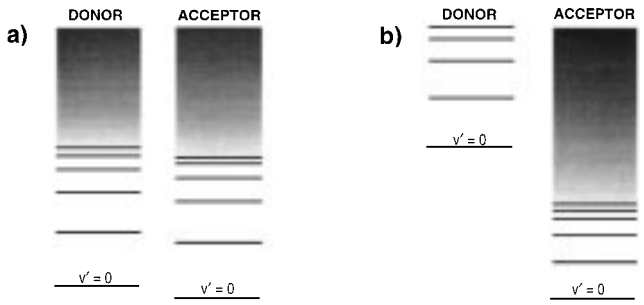

Figure 2. Schematic representation of the vibrational manifolds of the electronically excited states of the donor and the acceptor: (a) when the S_1^{DONOR}—$S_1^{ACCEPTOR}$ energy gap is small and comparable with the spacing of the lowest vibrational levels; (b) when the S_1^{DONOR}—$S_1^{ACCEPTOR}$ energy gap is much larger than the spacing between the vibrational levels.

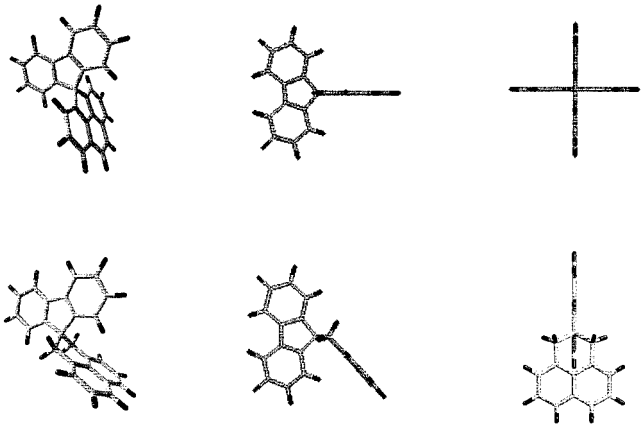

Figure 3. Three-dimensional views of the model compounds (spirofluorenephenanthrene (**SFP**) and spirofluorenenaphthalene (**SFN**). Note the C_{2v} symmetry of **SFP** and the C_s symmetry of **SFN**.

mutually orthogonal, and the higher order multipole interactions, as well as the exchange interaction, vanish by symmetry. We studied the new model compounds under supersonic expansion conditions to eliminate most fluctuations and sources of inhomogeneous line broadening that are present in condensed phases. It can be expected that increasing the energy gap between the donor and the acceptor may have a similar effect as populating vibrationally excited states of the donor in low energy gap compounds. As the energy gap increases, the vibrational ground state of the S_1 electronic excited state of the donor, $v_D = 0$, faces an increasing density of nearly degenerate vibrational states of the S_1 state of the acceptor (Figure 2b). The symmetry of some of these states will inevitably be appropriate for vibronic coupling and therefore excitation transfer. Thus, singlet energy transfer and emission from both chromophores can be expected when any vibronic state of the donor (including the zero-point vibrational level) is excited. In the limiting case of a very large energy gap (or "driving force" in the terminology of electron and excitation transfer in condensed phases), the situation will correspond to a coupling between a single well-defined donor state and a continuum of acceptor states. This is the classical setup of the Fermi "golden rule" describing nonradiative decay processes. There are two consequences of this situation. First, since intramolecular vibrational relaxation (IVR) proceeds much faster to the dense manifold of the acceptor, total quenching of the donor emission may occur. Second, absorption lines in the excitation spectrum corresponding to the Franck−Condon transitions of the donor will become broadened. Indeed, all large energy gap bichromophores in this study (diazospirobifluorene, dichlorospirobifluorene, spirofluorenephenanthrene, and spirofluorenenaphthalene) exhibit complete singlet energy transfer upon excitation of any donor state, and only acceptor fluorescence could be detected. Significant broadening of the donor excitation spectrum was observed in all cases. In the absence of an inhomogeneous contribution, there exists a direct link between the line width, ΔE, and the lifetime of the donor state, τ:

$$\tau \Delta E = \hbar \qquad (1)$$

When the radiative lifetime of the donor is long (as it is in the case of fluorene), τ is determined primarily by the rate of nonradiative energy transfer to the acceptor, $k_{EET} = 1/\tau$. Therefore, by simply measuring the width of the donor line, it is possible to establish the rate of electronic energy transfer. Since the behavior of all large energy gap model compounds was qualitatively identical, and because of space considerations, only the spectroscopy of two representative systems, the spirofluorenephenanthrene and the spirofluorenenaphthalene, will be discussed in full detail.

The presented findings demonstrate that the zero-order approach can overestimate the degree of the molecular orbital symmetry control over electronic excitation and charge-transfer rates. Even at rather modest magnitudes of the donor−acceptor energy gap (1500−4000 cm^{-1}), the "symmetry-forbidden" electronic energy transfer can occur on a picosecond time scale, thanks to efficient vibronic coupling. The presence of such strong vibronic interactions may explain why in all previously published cases the differences between the rates of the symmetry allowed and the symmetry forbidden exothermic charge-transfer reactions are much smaller than would have been expected from a zero-order localized molecular orbital picture.[2,5,6]

Experimental Section

A. Synthesis. *Spirofluorenephenanthrene (SFP).* 4,5-Methylenecyclophenanthrene [4H-cyclopenta[*def*]phenanthrene] (Lancaster, 98%) was oxidized nearly quantitatively to the corresponding ketone using the Jones reagent. The coupling of the ketone with the 2-bromobiphenyl (Lancaster, 98%) Grignard reagent and the subsequent ring closing were described previously.[3] The overall yield of these steps was ∼80%. The product was purified by recrystallization from a hexane/benzene mixture.

Spirofluorenenaphthalene (SFN). 1,8-Bis(bromomethyl)naphthalene was obtained in ∼70% by photoinitiated bromination of 1,8-dimethylnaphthalene (Fluka, 97%). A stoichiometric amount of a benzene/THF solution of the dibromide was added dropwise to the methanolic slurry of fluorene (Aldrich, 99%) with a slight excess of MeOLi (prepared in situ from lithium wire and MeOH). The product (∼70% yield) was purified by recrystallization from ethanol/hexane.

Dichlorospirobifluorene (2Cl−SBF). 2,7-Dibromofluorene (Lancaster, 97%) was converted to the 2,7-dichlorofluorene in a nearly quantitative yield via the classical $CuCl/CuCl_2$ halogen exchange reaction. The purified product was oxidized quantitatively to the 2,7-dichlorofluoren-9-one using the Jones reagent. The coupling of the 2,7-dichlorofluoren-9-one with the 2-bromobiphenyl Grignard reagent and the subsequent ring closing were described previously.[3] The overall yield of these steps was ∼80%. The product was purified by recrystallization.

All compounds were identified by NMR (300 MHz ^1H and 75 MHz ^{13}C), IR, and mass spectroscopy. The purity was assessed by NMR and thin-layer chromatography (TLC). In the case of dichlorospirobifluorene, the X-ray crystal structure was obtained.

The synthesis of the small energy gap spiranes (d_nh_{16-n}-spirobifluorene, $n = 0, 1, 2, 8$) and of the 4,5-diazospirobifluorene (**2N−SBF**) was already described in detail elsewhere.[3,7]

B. Spectroscopy. Both fluorescence excitation and dispersed fluorescence spectroscopy were used. Detailed descriptions of the experimental setup may be found elsewhere.[8] In brief, fluorescence excitation spectra were obtained by exciting samples entrained in a supersonic jet with the frequency-doubled output of a Nd:YAG pumped dye laser. The total fluorescence from the sample, as a function of the excitation frequency, was collected by *f*/1 optics that were orthogonal to both the excitation laser and the supersonic jet. To obtain a dispersed fluorescence spectrum, the excitation frequency was tuned to a resonance transition of the sample and the total fluorescence was dispersed either by a 1.0 m Spex monochromator equipped with a photomultiplier (RCA 8575) or a 0.275 m spectrograph (Acton Research Corporation, SpectraPro 275) to which a linear array detector (Princeton Applied Research, 1455B-700-HQ) was attached. To measure the fluorescence lifetime of a sample, the temporal profile of its fluorescence was captured by a Tektronix 2221 digital storage oscilloscope and the decay curve was transferred to a 486DX2/33MHz PC via a GPIB interface. Each decay curve was averaged over multiple laser pulses before the data were transferred.

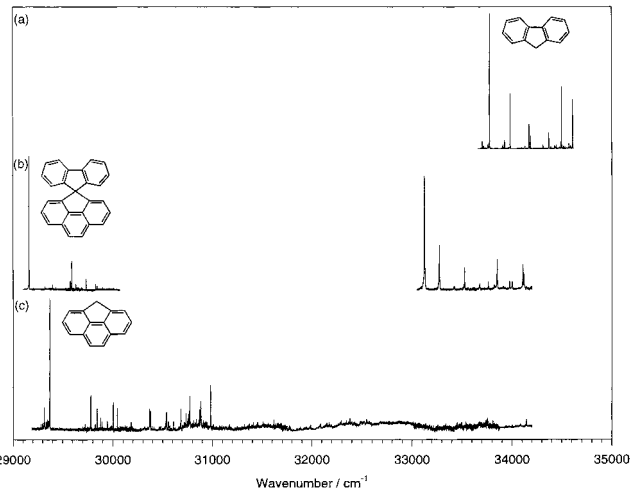

Figure 4. Fluorescence excitation spectra of (a) fluorene, (b) spirofluorenephenanthrene, and (c) cyclopentaphenanthrene. There are two spectral regions in (b) and the peak intensity in each region is only relative to the most intense peak of the same region, i.e., the S_{1P} and S_{1F} origin of cyclopentaphenanthrene at the low- and high-energy region, respectively.

Cyclopentaphenanthrene and spirofluorenephenanthrene were heated to 110 °C and 160−170 °C, respectively, and were entrained in helium at backing pressures of 30 and 50 psig, respectively. Dimethylnaphthalene was heated to 40 °C while spirofluorenenaphthalene was heated to 160−180 °C in order to obtain sufficient vapor pressure. To minimize the consumption of dimethylnaphthalene and spirofluorenenaphthalene, a helium backing pressure of only 10 psig was used. All sample molecules were seeded in helium and were expanded into a vacuum chamber through a 100 μm pinhole. With the continuous supersonic jet, the typical working pressure inside the vacuum chamber was kept below 25 mTorr. Cyclopentaphenanthrene, spirofluorenephenanthrene, and spirofluorenenaphthalene were prepared according to the method described in section A. Dimethylnaphthalene (95%) was purchased from Aldrich and was used as received.

Results

A. Cyclopentaphenanthrene. Figure 4c shows the fluorescence excitation spectrum of cyclopentaphenanthrene from 29200−34200 cm^{-1}. The spectrum is constructed by connecting seven excitation spectra together, and the relative intensities of adjacent spectra are scaled by overlapping features. This scaling method becomes inaccurate at high frequency since the peaks beyond 31 000 cm^{-1} are sparse and weak. Comparison of peak intensity is therefore not recommended. The spectral assignment of cyclopentaphenanthrene is given in Table 1. There is no previous report of the IR or Raman spectrum of cyclopentaphenanthrene to which we can refer, and our spectral assignment is mostly based on the harmonic vibrational frequencies computed from an AM1 optimized cyclopentaphenanthrene. In general, AM1 provides a more reliable geometry prediction over other semiempirical methods.[9] As a result of anharmonic corrections, quantum mechanical calculations systematically overestimated harmonic vibrational frequencies. In the case of AM1, a 10.4% error is expected.[10]

TABLE 1: Vibronic Transitions Assignment in the First 2000 cm^{-1} of the $S_1 \leftarrow S_0$ Excitation Spectrum of Cyclopentaphenanthrene

position/cm^{-1}	shift[a]/cm^{-1}	intensity	assignment[b]	AM1[c]
29 370	0	vs	origin	
29 723	353	mw	$a_2 \cdot a_2$	360
29 780	410	s	a_1	376
29 844	474	ms	a_1	474
29 877	507	m	$b_1 \cdot b_1$	508
29 893	523	m	b_2	522
29 944	574	m	b_2	570
30 004	634	s	b_2	595
30 043	673	ms	a_1	659
30 369	999	ms	474 + 523	
30 379	1009	ms	b_2	1125
30 414	1044	mw	2 × 523	
30 468	1098	mw	523 + 574	
30 520	1150	mw	2 × 574	
30 535	1165	ms	a_1	1158
30 540	1170	ms	b_2	1164
30 553	1183	w	410 + 673	
30 558	1188	m	a_1	1201
30 571	1201	mw	b_2	1230
30 609	1239	m	a_1	1233
30 677	1307	m	634 + 673	
30 684	1314	ms	b_2	1325
30 718	1348	mw	2 × 673	
30 722	1352	w	a_1	1340
30 734	1364	m	353 + 1009	
30 749	1379	mw	a_1	1377
30 755	1385	m		
30 775	1405	s	410 + 999	
30 812	1442	mw	a_1	1442
30 839	1469	mw	474 + 999	
30 873	1503	m	b_2	1482
30 881	1511	m	b_2	1511
30 887	1517	ms	353 + 1165	
30 982	1612	s	a_1	1609
31 616	2246	mw	634 + 1612	

[a] Vibrational frequencies are blue-shifted with respect to the origin at 29 370 cm^{-1}. [b] Assignment based on C_{2v} symmetry. [c] S_0 vibrational frequencies calculated from AM1 optimized cyclopentaphenanthrene.

There are some hot band transitions lying within 150 cm^{-1} to the red of the 29 370 cm^{-1} S_1 origin, probably due to insufficient cooling of some twisting modes associated with the cyclopentyl ring. Since the origin is the most intense feature, the geometry of cyclopentaphenanthrene in the S_1 state is similar to that in the ground state. Most of the S_1 vibronic activity is confined within the first +2000 cm^{-1}. Beyond 31 000 cm^{-1}, the spectrum is dominated by weak and sharp transitions that are sitting on top of a broad and slightly absorbing background. At high vibronic energy, unfavorable Franck−Condon factors can weaken the absorption cross section whereas the onset of IVR can significantly broaden a transition and turn adjacent transitions into a broad band. In addition to the totally symmetric a_1 vibrations, many b_2 vibrations are observed. These b_2 transitions probably gain their intensities by vibronic coupling to a low-lying S_2 state with B_2 symmetry. This S_2 state is most likely located at ∼+5600 cm^{-1} in cyclopentaphenanthrene and resembles the ∼+6000 cm^{-1} S_2 state observed in phenanthrene.[11−13]

In Figure 5b, we show the emission spectrum of cyclopentaphenanthrene excited at the S_1 origin. Most features can be assigned to a_1 and b_2 fundamentals plus combination bands containing the 1475 cm^{-1} b_2 fundamental. The spectral assignment of the emission spectrum is listed in Table 2. The strong 0−0 emission shows that the geometry of cyclopentaphenanthrene is similar in S_0 and S_1, which is quite reasonable in view of the rigidity of cyclopentaphenanthrene.

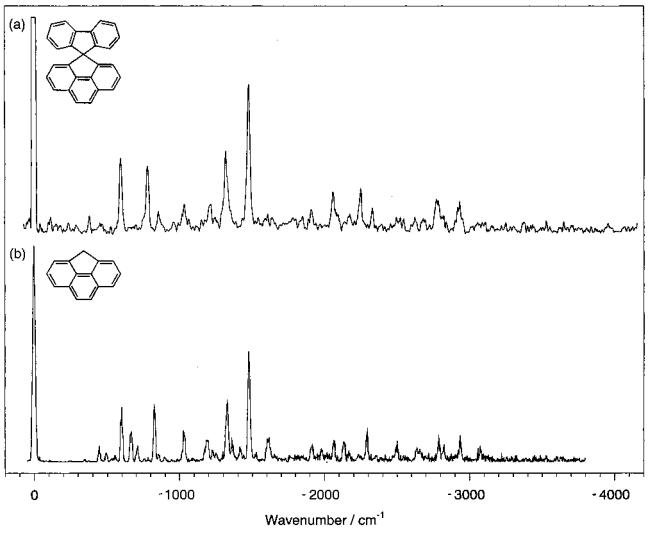

Figure 5. Single vibronic level emission spectra of (a) spirofluorenephenanthrene at 29 164 cm^{-1} (S_{1P}) and (b) cyclopentaphenanthrene at 29 370 cm^{-1} (S_1). The spectral resolution is 20 cm^{-1} in both spectra.

TABLE 2: Assignment of the SVL Emission of Cyclopentaphenanthrene Excited at the S_1 Origin

position/cm^{-1}	shift[a]/cm^{-1}	intensity	assignment[b]	S_1[c]	S_0[d]
29 370	0	vs	origin		
29 022	348	vw	$a_2 \cdot a_2$	353	250
29 926	444	mw	a_1	410	406
29 880	490	mw	a_1	474	
29 815	555	w	b_2	523, 574	540
29 770	600	ms	b_2	634	
29 706	664	ms	a_1	673	
29 660	710	mw	b_2	755[e]	710
29 544	826	ms	a_1	812[e]	830
29 515	855	w	b_2	864[e]	
29 475	895	vw	2 × 444		
29 342	1028	m	b_2	1009	1038
29 176	1194	m	a_1	1165	1200
29 146	1224	w	b_2	1201	
29 118	1252	vw	a_1	1239	1244
29 045	1325	ms	b_2	1314	1303
29 012	1358	mw	a_1	1379	1365
27 953	1417	mw	600 + 826		1417
27 895	1475	s	b_2	1503	1441
27 840	1530	vw	710 + 826		1524
27 765	1605	m	a_1	1612	1608
27 458	1912	mw	444 + 1475		
27 392	1978	w	490 + 1475		
27 308	2062	mw	600 + 1475		
27 237	2133	mw	664 + 1475		
27 200	2170	vw	710 + 1475		
27 073	2297	m	826 + 1475		
26 875	2495	mw	1028 + 1475		
26 713	2657	mw	1194 + 1475		
26 582	2788	mw	1325 + 1475		
26 545	2825	w	1358 + 1475		
26 433	2937	mw	2 × 1475		
26 297	3073	w	1605 + 1475		

[a] Vibrational frequencies are red-shifted with respect to the origin at 29 370 cm^{-1}. [b] Assignment based on C_{2v} symmetry. [c] Correlation with S_1 vibronic transitions. [d] Ground-state vibrational frequencies of phenanthrene from ref 13. [e] S_0 vibrational frequencies calculated from AM1 optimized cyclopentaphenanthrene.

B. Spirofluorenephenanthrene. We compare the fluorescence excitation spectrum of spirofluorenephenanthrene in Figure 4b with those of the two model compounds, fluorene and cyclopentaphenanthrene, in parts a and c of Figure 4, respectively. In Figure 4b, we focus on two spectral regions

TABLE 3: Vibronic Transitions Assignment in the First 1000 cm^{-1} of the $S_{1N} \leftarrow S_0$ Excitation Spectrum of Spirofluorenephenanthrene

position/cm^{-1}	shift[a]/cm^{-1}	intensity	assignment[b]	S_1[c]	S_1[d]
29 164	0	vs	origin		
29 203	39	vw	twist/bend		43
29 322	158	w	twist/bend		141, 142
29 398	234	mw	twist/bend		232
29 432	268	w	twist/bend		247
29 576	412	m	a_1	410	
29 591	427	ms	twist/bend		418
29 633	469	mw	a_1	474	
29 734	570	m	b_2	574	
29 831	667	mw	b_2	634	
29 849	685	w	a_1	673	
29 898	734	vw	268 + 469		
30 006	842	vw	412 + 427		

[a] Vibrational frequencies are blue-shifted with respect to the origin at 29 164 cm^{-1}. [b] Assignment based on C_{2v} symmetry. [c] Correlation with S_1 vibronic transitions of cyclopentaphenanthrene. [d] Correlation with S_1 intramolecular modes of spirobifluorene.

TABLE 4: Vibronic Transitions Assignment in the First 1000 cm^{-1} of the $S_{1F} \leftarrow S_0$ Excitation Spectrum of Spirofluorenephenanthrene

position/cm^{-1}	shift[a]/cm^{-1}	intensity	assignment[b]	S_1[c]
33 124	0	vs	origin	
33 270	146	ms	?	150
33 274	150	s	a_1	205
33 422	298	w	2 × 150	
33 528	404	ms	a_1	395
33 673	549	w	146 + 404	
33 678	554	mw	150 + 404	
33 763	639	m	b_2	593
33 824	700	mw	298 + 404	
33 852	728	ms	a_1	721
33 913	789	w	150 + 639	
33 929	805	vw	2 × 404	
33 977	853	m	a_1	832
34 002	878	m	150 + 728	
34 109	985	ms	a_1	985
34 121	997	ms	?	

[a] Vibrational frequencies are blue-shifted with respect to the origin at 33 124 cm^{-1}. [b] Assignment based on C_{2v} symmetry. [c] Correlation with S_1 vibronic transitions of fluorene.

where the initial excitation is localized either at the low-energy phenanthrene side or the high-energy fluorene side. We designate the first excited spirofluorenephenanthrene state localized on the phenanthrene side as the S_{1P} state and the first excited spirofluorenephenanthrene state localized at the fluorene side as the S_{1F} state. The spectral assignment of spirofluorenephenanthrene is given in Tables 3 and 4. The S_{1P} origin of spirofluorenephenanthrene is located at 29 164 cm^{-1}, a spectral shift of −206 cm^{-1} relative to cyclopentaphenanthrene. The S_{1F} origin is at 33 124 cm^{-1}, a spectral shift of −653 cm^{-1} relative to fluorene.

In parts a and b of Figures 6, we compare the fluorescence excitation spectra of spirofluorenephenanthrene and cyclopentaphenanthrene in the S_{1P} region. The hot bands in cyclopentaphenanthrene have completely disappeared in spirofluorenephenanthrene. The attachment of a fluorene unit to cyclopentaphenanthrene creates low-frequency vibrational modes that can help cool the higher frequency modes through collision-induced IVR. The emission spectra of spirofluorenephenanthrene and cyclopentaphenanthrene in Figure 5 are so similar that both of them can be assigned to a_1 and b_2 fundamentals and combination bands containing an active 1475 cm^{-1} mode. This indicates that the energy level structure of cyclopentaphenanthrene remains

TABLE 5: Assignment of the SVL Emission of Spirofluorenephenanthrene Excited at the S_{1P} Origin

position/cm^{-1}	shift[a]/cm^{-1}	intensity	assignment[b]	S_0[c]
29 164	0	vs	origin	
29 038	114	w	twist/bend	
28 774	378	w	a_1	444
28 549	592	ms	b_2	600
28 371	780	ms	a_1	826
28 298	854	mw	b_2	855
28 123	1033	mw	b_2	1028
27 941	1215	mw	2 × 592	
27 838	1318	ms	b_2	1325
27 677	1475	s	b_2	1475
27 235	1912	w	592 + 1318	
27 094	2056	m	592 + 1475	
26 978	2174	vw	854 + 1318	
26 905	2248	m	780 + 1475	
26 823	2329	mw	854 + 1475	
26 366	2770	m	1318 + 1475	
26 220	2932	m	2 × 1475	

[a] Vibrational frequencies are red-shifted with respect to the origin at 29 164 cm^{-1}. [b] Assignment based on C_{2v} symmetry. [c] Correlation with the $S_1 \rightarrow S_0$ vibronic transitions of cyclopentaphenanthrene.

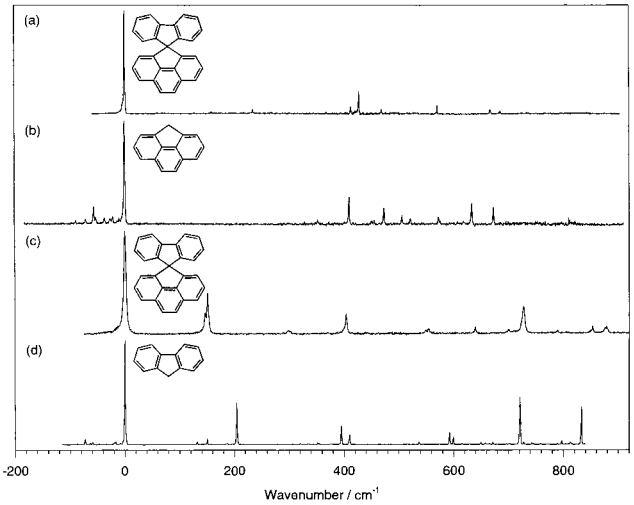

Figure 6. The first 1000 cm^{-1} fluorescence excitation spectrum of (a) spirofluorenephenanthrene at 29 164 cm^{-1} (S_{1P}), (b) cyclopentaphenanthrene at 29 370 cm^{-1} (S_1), (c) spirofluorenephenanthrene at 33 124 cm^{-1} (S_{1F}), and (d) fluorene at 33 777 cm^{-1} (S_1).

almost undisturbed in spirofluorenephenanthrene. The spectral assignment of the S_{1P} emission spectrum is given in Table 5.

We compare the fluorescence excitation spectra of fluorene and spirofluorenephenanthrene in the S_{1F} region in parts c and d of Figure 6. The corresponding spectral assignment is given in Table 4. The S_{1F} excitation spectrum of spirofluorenephenanthrene in the first 1000 cm^{-1} is dominated by a_1 transitions, with only a single transition assigned to b_2 symmetry. The 205 cm^{-1} mode in fluorene is reduced to 150 cm^{-1} in spirofluorenephenanthrene, compared to 212 cm^{-1} in spirobifluorene.[3] This assignment is based on their similar propensities to form combination bands with other vibrational modes. Except for the 150 cm^{-1} mode, most vibrations in spirofluorenephenanthrene have frequencies close to the corresponding vibrations of fluorene.

The emission spectra of spirofluorenephenanthrene excited at different excess energies above the S_{1F} origin are shown in Figure 7. There is no detectable emission in the first −3000 cm^{-1} and the emission is red-shifted ∼4000 cm^{-1} from the S_{1F} origin. These spectra contain broad emission bands with the first feature in every spectrum located at ∼29 164 cm^{-1}, the S_{1P} origin of spirofluorenephenanthrene. For comparison, we

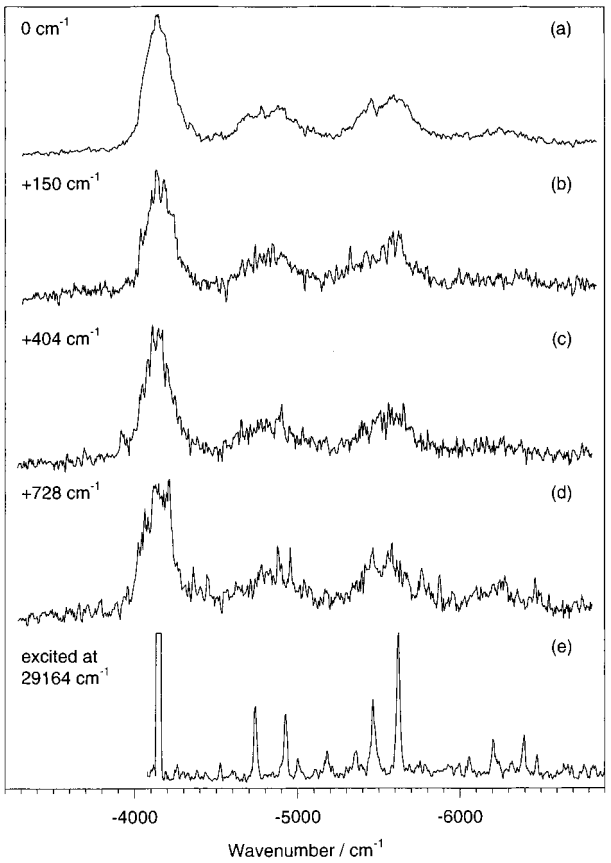

Figure 7. Single vibronic level emission spectra of spirofluorenephenanthrene excited at (a) 33 124 cm^{-1} (S_{1F}), (b) +150 cm^{-1}, (c) +404 cm^{-1}, and (d) +728 cm^{-1}. (e) Single vibronic level emission spectrum of spirofluorenephenanthrene excited at 29 164 cm^{-1} (S_{1P}). The spectral resolution is 100 cm^{-1} in (a−d) and 20 cm^{-1} in (e). The abscissa applies to (a−d) only; it does not apply to (e).

reproduce the emission spectrum of the S_{1P} origin in Figure 7e. Except for the broadening, the S_{1F} and S_{1P} emission spectra in Figure 7 are similar. Electronic energy transfer occurs in the S_{1F} state of spirofluorenephenanthrene and excitation to the fluorene unit produces fluorescence exclusively from the phenanthrene unit. The rate of electronic energy transfer is so fast that the transfer of excitation energy is complete before the initially excited fluorene unit has a chance to emit.

C. 1,8-Dimethylnaphthalene. The jet spectroscopy of dimethylnaphthalene was first studied by Chakraborty and Chowdhury.[14] Our measurements agree fairly well with theirs; however, we revise some of their spectral assignments. We extend the measurement of dimethylnaphthalene well beyond its S_2 origin as shown in Figure 8c. The spectrum covers 5500 cm^{-1} continuously from 31200 to 36700 cm^{-1}. The spectrum is again constructed from several excitation spectra. The scaling method works well in dimethylnaphthalene since there are many sharp and moderately intense transitions across the 5500 cm^{-1} spectral region.

The most intense peak is the S_1 origin, and low-frequency vibrations are obvious within the first 100 cm^{-1} of the S_1 origin, probably due to torsional motions associated with the two methyl groups. Like naphthalene, the excitation spectrum of dimethylnaphthalene is dominated by a_1 and b_2 modes. Most vibronic activity is confined to the first 1500 cm^{-1} with only a few bands extending to the S_2 region. On the basis of the excitation spectrum, the relatively strong transition at 34 384 cm^{-1} (+3040 cm^{-1} from the S_1 origin) is likely to be the S_2 origin. This S_2-S_1 gap is +3900 cm^{-1} in naphthalene.[15,16] Possibly the S_2 origin

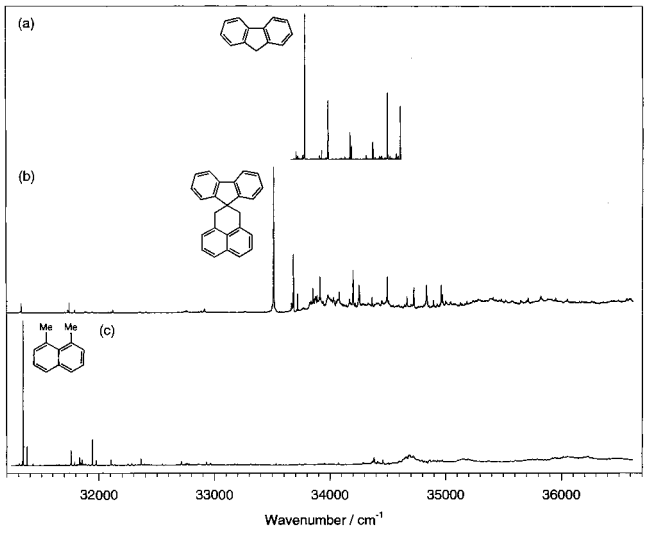

Figure 8. Fluorescence excitation spectrum of (a) fluorene, (b) spirofluorenenaphthalene, and (c) 1,8-dimethylnaphthalene.

TABLE 6: Vibronic Transitions Assignment of the $S_1 \leftarrow S_0$ Spectrum of 1,8-Dimethylnaphthalene

position/cm^{-1}	shift[a]/cm^{-1}	intensity	assignment[b]	S_1[c]	S_1[d]
31 341	0	vs	origin		
31 374	33	s	CH_3-torsion	33	
31 426	85	mw	CH_3-torsion	88	
31 760	419	s	$\bar{8}_0^1$	428	419
31 790	449	m	33 + 419	459	
31 833	492	ms	9_0^1	500	484
31 856	515	ms		515	
31 868	527	mw	33 + 492		
31 945	604	s	8_0^1	613	661
31 977	636	ms	33 + 604	647	
32 105	764	ms	$\bar{7}_0^1$	758	815
32 139	798	w	33 + 764		
32 251	910	mw	$\bar{8}_0^1 9_0^1$	914	
32 284	943	m	$\bar{8}_0^1 8_0^1$	943	970
32 317	976	w	33 + 943		
32 364	1023	ms	8_0^2	1021	
32 397	1056	mw	33 + 1023		
32 547	1206	mw	8_0^2	1204	
32 712	1371	m	$\bar{7}_0^1 8_0^1$	1370	
32 930	1589	m	$\bar{8}_0^1 6_0^1$	1590	1579[e]
32 968	1627	m	$\bar{8}_0^1 8_0^2$		
33 532	2191	mw	$\bar{8}_0^1 8_0^1 6_0^1$		
33 735	2394	mw			
33 952	2611	mw	$\bar{6}_0^1 4_0^1$		2603[e]
34 073	2732	mw			2773[e]
34 384	3043	ms	$\bar{7}_0^1 8_0^1 4_0^1$		3046[e]
34 417	3076	m	$\bar{4}_0^1 9_0^2 8_0^1$		3076[e]
34 459	3118	ms	$\bar{7}_0^1 9_0^3 8_0^1$		3111[e]
34 599	3258	m			
34 658	3317	ms			
34 688	3347	ms			
34 717	3376	ms			

[a] Vibrational frequencies are blue-shifted with respect to the origin at 31 341 cm^{-1}. [b] Convention based on ref 28. [c] Measurements made in ref 14. [d] Measurements made in ref 12. [e] Measurements made in ref 15.

of dimethylnaphthalene lies between 34200 and 34800 cm^{-1}. The humps that begin at 34 700 cm^{-1} resemble those observed in the S_2 region of naphthalene. The spectral assignment of dimethylnaphthalene is given in Table 6.

In naphthalene, $S_0 \leftrightarrow S_1$ is a symmetry-allowed transition, yet this transition has a very small oscillator strength to the

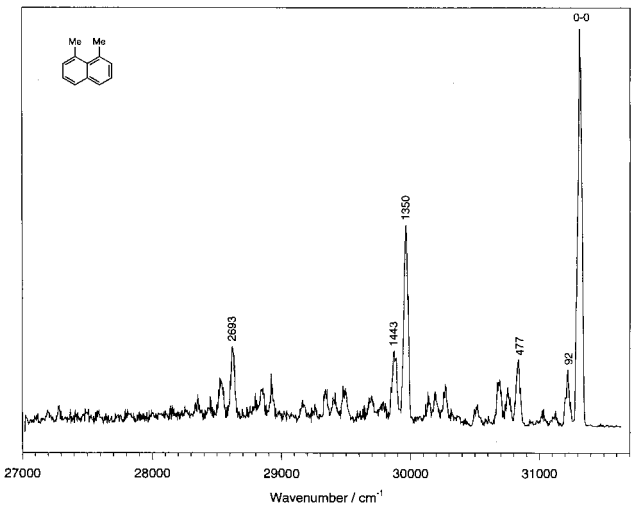

Figure 9. Single vibronic level emission spectrum of 1,8-dimethylnaphthalene excited at 31 341 cm^{-1} (S_1). The spectral resolution is 40 cm^{-1}.

ground state. This is because of an accidental cancellation of the S_1 transition moment due to configuration interactions of low-lying excited states.[15,16] The S_2 origin in naphthalene is ~20 times stronger than the S_1 origin, leaving the bulk of the S_1 spectrum borrowing intensity from the S_2 state via vibronic coupling. This delicate cancellation of the transition moment is vulnerable to the breaking of symmetry induced by chemical substitutions. The S_1 origin of dimethylnaphthalene is almost an order of magnitude more intense than the S_2 origin. This same effect has also been reported in various mono- and disubstituted naphthalene derivatives.[17−19]

The emission spectrum of dimethylnaphthalene is shown in Figure 9. The emission spectrum is dominated by a_1 and b_2 fundamentals and combinations containing an active 1350 cm^{-1} a_1 mode. The spectral assignment is given in Table 7.

D. Spirofluorenenaphthalene. Figure 8b shows the fluorescence excitation spectrum of spirofluorenenaphthalene. The spectrum contains two parts with very different intensity distributions. The low-energy part (below 33 500 cm^{-1}) with a weaker transition moment is naphthalene-like. The high-energy part (33 500 cm^{-1} and above) with a much stronger transition moment has fluorene-like absorptions sitting on top of a broad background that begins near 33 800 cm^{-1}. The excitation spectrum of spirofluorenenaphthalene looks very much like a superposition of a dimethylnaphthalene and a fluorene spectrum with some spectral shifts. We assign the peaks at 31 325 and 33 512 cm^{-1} as the S_{1N} and S_{1F} origins of spirofluorenenaphthalene with the initial excitation localized at the naphthalene and fluorene unit, respectively. The broad background that begins at 33 800 cm^{-1} is most likely the S_2 origin belonging to the naphthalene unit. We assign this as the S_{2N} state of spirofluorenenaphthalene.

A comparison between spirofluorenenaphthalene and dimethylnaphthalene at S_{1N} is shown in parts a and b of Figure 10. While dimethylnaphthalene shows some torsional activity of the two methyl groups, spirofluorenenaphthalene exhibits none since the two methyl groups are linked together via a carbon atom in spirofluorenenaphthalene. In dimethylnaphthalene, torsional motions of the methyl groups are free and are decoupled from the ring modes. In spirofluorenenaphthalene, these same torsional motions are arrested by coupling to the ring modes. As a consequence, these low-frequency torsional modes mix with the ring modes and produce a fairly complicated excitation

TABLE 7: Assignment of the SVL Emission of 1,8-Dimethylnaphthalene Excited at the S_1 Origin

position/cm^{-1}	shift[a]/cm^{-1}	intensity	assignment[b]	S_1[c]
31 341	0	vs	origin	0
31 249	92	ms	CH_3-torsion	85
31 154	187	vw	2×92	
31 054	287	vw	?	
30 864	477	ms	$\bar{8}_1^0$	419
30 781	560	mw	9_1^0	492
30 723	618	m	8_0^1	604
30 549	792	w	$\bar{7}_1^0$	764
30 303	1038	m	$\bar{8}_1^0 9_1^0$	
30 226	1115	mw	9_2^0	
30 170	1171	mw	$9_1^0 8_1^0$	
29 991	1350	s	5_1^0	
29 898	1443	ms	$92 + 1350$	
29 725	1616	mw	$287 + 1350$	
29 508	1833	mw	$\bar{8}_1^0 5_1^0$	
29 449	1892	mw	$9_1^0 5_1^0$	
29 371	1970	mw	$8_1^0 5_1^0$	
28 954	2387	m	$\bar{8}_1^0 9_1^0 5_1^0$	
28 878	2463	mw	$9_1^0 5_1^0$	
28 827	2514	mw	$9_1^0 8_1^0 5_1^0$	
28 648	2693	ms	5_2^0	
28 555	2786	m	$92 + 2693$	
28 384	2967	mw	$287 + 2693$	

[a] Vibrational frequencies are red-shifted with respect to the origin at 31 341 cm^{-1}. [b] Convention based on ref 28. [c] Correlation with S_1 vibronic transitions of 1,8-dimethylnaphthalene.

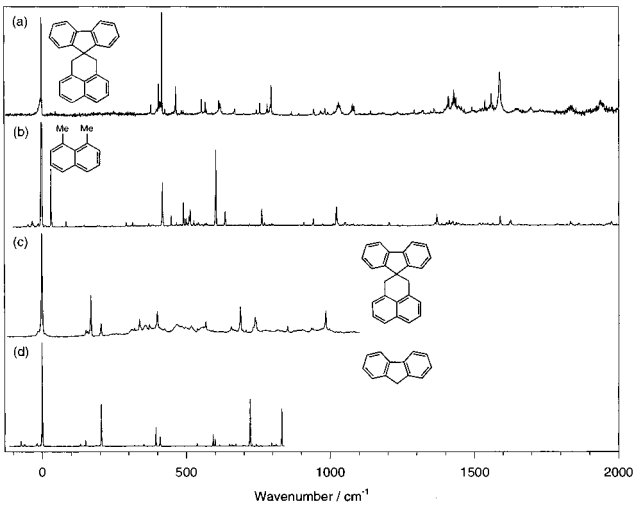

Figure 10. The first 2000 cm^{-1} fluorescence excitation spectrum of (a) spirofluorenenaphthalene at 31 325 cm^{-1} (S_{1N}) and (b) 1,8-dimethylnaphthalene at 31 341 cm^{-1} (S_1). The first 1000 cm^{-1} fluorescence excitation spectrum of (c) spirofluorenenaphthalene at 33 512 cm^{-1} (S_{1F}) and (d) fluorene at 33 777 cm^{-1} (S_1).

spectrum. This is the reason for the difference between the two spectra in Figure 10. In general, Figure 10a looks more like the excitation spectrum of acenaphthalene in which the two methyl groups are directly linked to each other.[14] In this study, the naphthalene unit in spirofluorenenaphthalene serves as an intermediate case between the rigid acenaphthalene and the relatively free dimethylnaphthalene. The S_{1N} state spectral assignment is listed in Table 8. The excitation spectrum of the first 1100 cm^{-1} into the S_{1F} region of spirofluorenenaphthalene is compared with the S_1 spectrum of fluorene in parts c and d of Figure 10, and the complete spectral assignment is presented in Table 9.

Excitation to the S_{1F} state leaves the bichromophore locally excited on the fluorene side only. Figure 11 shows a series of emission spectra at different excess energies above the S_{1F}

TABLE 8: Vibronic Transitions Assignment in the First 2000 cm^{-1} of the $S_{1N} \leftarrow S_0$ Excitation Spectrum of Spirofluorenenaphthalene

position/cm^{-1}	shift[a]/cm^{-1}	intensity	assignment[b]	S_1[c]	AM1[d]
31 325	0	vs	origin		
31 704	379	m	2 × 189	356	2 × 186
31 730	405	ms	b_2	399	406
31 742	417	vs	$b_2(\bar{8}_0^1)$	413	459
31 751	426	w	a_1	426	439
31 790	465	ms	$a_1(9_0^1)$	424	467
31 810	485	w	a_1		482
31 817	492	w	b_2		504
31 880	555	m	a_1		561
31 892	567	m	3 × 189		
31 939	614	m	a_1	603	560
31 944	619	m	$a_1(8_0^1)$	608	639
31 994	669	mw	a_1	684	
32 070	745	mw	$b_2(\bar{7}_0^1)$	738	
32 082	757	m	4 × 189		
32 108	783	m	379 + 405	775	766
32 121	796	ms	379 + 417	793	810
32 129	804	vw	379 + 426		
32 193	868	w	a_1/b_2		868/871
32 218	893	w	$a_1(7_0^1)$		918
32 270	945	mw	5 × 189	950	
32 294	969	mw	417 + 555	970	
32 298	973	mw	405 + 567	978	
32 309	984	mw	417 + 567	987	
32 318	993	mw	426 + 567	997	
32 355	1030	m	465 + 567	1032	
32 370	1045	w	379 + 669		
32 403	1078	m	465 + 614	1041	
32 408	1083	m	465 + 619	1059	
32 466	1141	mw	b_2	1185	1143
32 736	1411	m	465 + 945	1421	
32 754	1429	ms	669 + 757	1428	
32 762	1437	m	405 + 1030	1439	
32 771	1446	mw	417 + 1030	1469	
32 781	1456	mw	669 + 783	1476	
32 913	1588	s	$b_2(\bar{8}_0^1 6_0^1)$	1581	

[a] Vibrational frequencies are blue-shifted with respect to the origin at 31 325 cm^{-1}. [b] Assignment based on C_{2v} symmetry. Correlation to S_1 vibronic transitions of 1,8-dimethylnaphthalene is enclosed in parentheses. [c] Measurements made in ref 14. [d] S_0 vibrational frequencies calculated from AM1 optimized 2,3-dihydrophenalene.

origin. In all cases, the emission is naphthalene-like. Also shown in Figure 11f is the emission spectrum of dimethylnaphthalene from its S_1 origin. The emission spectra show essentially complete energy transfer.

Discussion

A. Cyclopentaphenanthrene/Spirofluorenephenanthrene System. In electronic energy transfer in spirofluorenephenanthrene, fluorene is the donor and phenanthrene is the acceptor. As in the previously studied case of spirobifluorene, the planes of the two chromophores are perpendicular and this places symmetry restrictions on the mechanism responsible for energy transfer.[3] The $S_1 \leftrightarrow S_0$ transition moment of fluorene is polarized along the long axis, whereas the $S_1 \leftrightarrow S_0$ and $S_2 \leftrightarrow S_0$ transition moments of phenanthrene are both in-plane and are polarized along the short and long axes, respectively.[11] Because the transition moments of fluorene and phenanthrene are perpendicular, energy transfer via dipolar coupling is forbidden as long as the symmetry is maintained.[20,21] Because the π systems of the two rings are orthogonal, exchange-coupled energy transfer is also forbidden in the symmetric molecule.[22]

In the case of spirobifluorene, coupling between the initially excited donor vibronic level and nontotally symmetric vibronic levels of the bichromophore will allow vibrationally induced electronic energy transfer. In d_8h_8-spirobifluorene, the energy gap between the two chromophores was 106 cm^{-1}, and at low vibrational excitation, efficient energy transfer depended on accidental coincidences between donor and acceptor vibronic levels.[3]

TABLE 9: Vibronic Transitions Assignment in the First 1500 cm^{-1} of the $S_{1F} \leftarrow S_0$ Excitation Spectrum of Spirofluorenenaphthalene

position/ cm^{-1}	shift[a]/ cm^{-1}	intensity	assignment[b]	S_1[c]	S_1[d]	S_1[e]
33 512	0	vs	origin			
33 664	152	mw	? b_1	150	146	119
33 670	158	mw	twist/bend			
33 681	169	s	a_1	205	150	210
33 716	204	ms	? b_1			222
33 832	320	mw	152 + 169			
33 850	338	m	2 × 169			
33 870	358	mw	152 + 204			
33 886	374	mw	169 + 204			
33 912	400	ms	a_1	395	404	399
34 051	539	w	b_2	537		542
34 080	568	m	169 + 400			
34 169	657	mw	b_2	593	639	601
34 200	688	s	? b_1			683
34 220	708	mw	169 + 539			
34 250	738	ms	a_1	721	728	725
34 365	853	m	a_1	832	853	834
34 497	985	ms	a_1	985	985	985
34 510	998	w	b_2		997	977
34 665	1153	m	169 + 985			
34 725	1213	ms	a_1		1231	1227
34 832	1320	ms	a_1			1321
34 960	1448	ms	a_1			1457
34 971	1459	m	a_1			1532

[a] Vibrational frequencies are blue-shifted with respect to the origin at 33 512 cm^{-1}. [b] Assignment based on C_{2v} symmetry. [c] Correlation with S_1 vibronic transitions of fluorene. [d] Correlation with S_{1F} vibronic transitions of spirofluorenephenanthrene. [e] Fluorene vibronic measurements made in ref 28.

The energy gap is 3960 cm^{-1} in spirofluorenephenanthrene. When the S_{1F} state is initially excited, those S_{1P} vibronic levels that are isoenergetic to the S_{1F} state are left unexcited due to poor Franck−Condon factors. This gives a fluorene-like excitation spectrum. As in the case for spirobifluorene, vibronic coupling in spirofluorenephenanthrene allows energy transfer from fluorene to phenanthrene. This vibrationally induced electronic energy transfer is induced by nontotally symmetric vibrations that break the symmetry of the bichromophore (e.g., interchromophoric scissoring, wagging, and bending modes). With the 3960 cm^{-1} energy gap in spirofluorenephenanthrene, the density of states of the acceptor is high enough that energy transfer no longer depends on accidental coincidences even at the zero-point energy level of the S_{1F} state. Our observation that only phenanthrene-like fluorescence is observed when any fluorene-like level is excited indicates that energy transfer is fast compared to the radiative decay rate of fluorene.

The efficient energy transfer in spirofluorenephenanthrene also lengthens the fluorescence lifetime over that of fluorene. We measured the fluorescence lifetime of fluorene to be 16.7 ± 0.8 ns, that of cyclopentaphenanthrene to be 61.3 ± 5.1 ns, and that of spirofluorenephenanthrene excited at the S_{1F} origin to be 49.0 ± 0.9 ns. The fluorescence lifetime of phenanthrene is 78 ns.[11]

The electronic energy transfer reported in this paper is in the statistical limit of radiationless transitions where a single donor state is coupled to numerous isoenergetic acceptor states.[23−25] This leads to irreversible electronic energy transfer after excitation of the donor and spectral broadening in the absorption

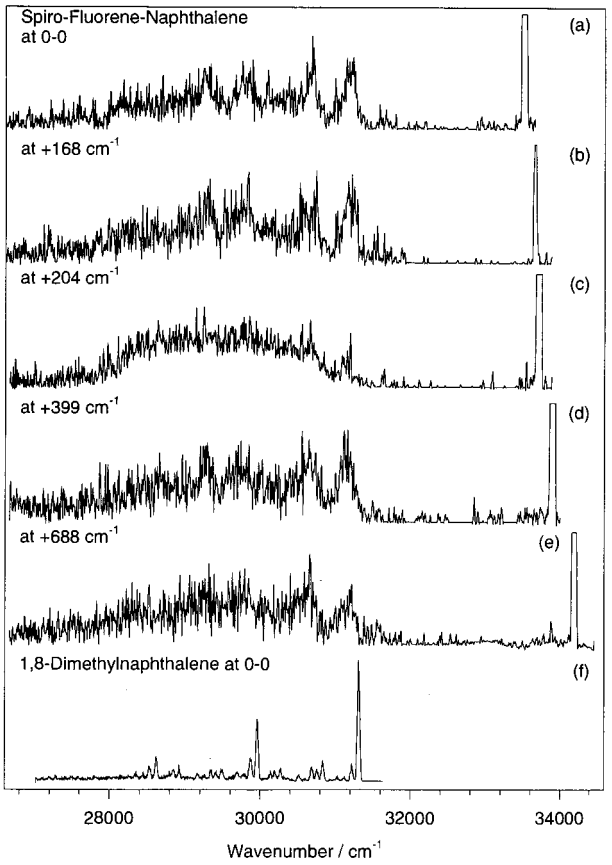

Figure 11. Single vibronic level emission spectra of spirofluorenenaphthalene excited at (a) 33 512 cm^{-1} (S_{1F}), (b) +168 cm^{-1}, (c) +204 cm^{-1}, (d) +399 cm^{-1}, and (e) +688 cm^{-1}. (f) Single vibronic level emission spectrum of 1,8-dimethylnaphthalene excited at 31 341 cm^{-1} (S_{1N}). The sharp peaks at high energy in (a−e) are scattered light from the excitation laser. The spectral resolution is 40 cm^{-1} in all spectra.

spectrum due to a shorter excited-state lifetime. Each donor absorption peak will have a Lorentzian line shape with a width that is determined by the rate of electronic energy transfer. If the observed line width (fwhm) Δ_{DA} is produced by a homogeneous Lorentzian line width (fwhm), Γ, and a Gaussian heterogeneous line width (fwhm), Δ_D, the observed line shape is a convolution of a Gaussian with a Lorentzian known as a Voight profile.

$$I(x) = \frac{1}{\sqrt{\pi}\eta}\int_{-\infty}^{\infty}\frac{\exp[-(x-y)^2/\eta^2]}{1+y^2}\,dy \qquad (2)$$

In this formula, η is Δ_D/Γ, the ratio of the Gaussian to Lorentzian line widths. A formula giving the homogeneous line width (fwhm), Γ, of a vibronic peak broadened by radiationless transitions in terms of the observed line width of the peak, Δ_{DA}, and the observed line width in the absence of the radiationless transition, Δ_D, was given by Amirav et al.[26] This model assumed that in the absence of radiationless transitions, the line shape was Gaussian and the width was produced by heterogeneous broadening, either unresolved rotational structure or laser bandwidth. The Amirav et al. model corrects for this heterogeneous broadening. For bichromophores, the correction is given by

$$\Gamma = [\Delta_{DA}{}^2 - [\Delta_D{}^2/(2\ln 2)]\}/\Delta_{DA} \qquad (3)$$

In Figure 12, we compare the absorption profile of the S_{1F} origin

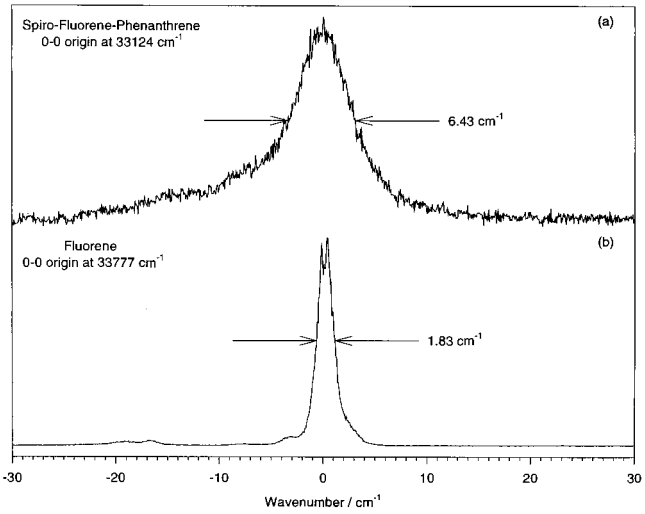

Figure 12. The fluorescence excitation profile of (a) the S_{1F} origin of spirofluorenephenanthrene and (b) the S_1 origin of fluorene.

of spirofluorenephenanthrene to the S_1 origin of fluorene. The fwhm of fluorene is 1.83 cm^{-1}, which is presumably due to the heterogeneious broadening. The fwhm of spirofluorenephenanthrene is 6.43 cm^{-1}. By numerically evaluating the width of the Voight line shape,[27] we extract a homogeneous line width of 5.88 cm^{-1} or $k_{EET} = 1.11 \times 10^{12}$ s^{-1} ($\tau_{EET} = 0.90$ ps), which is 4 orders of magnitude shorter than the fluorescence lifetime of fluorene.

B. Dimethylnaphthalene/Spirofluorenenaphthalene System. In electronic energy transfer in spirofluorenenaphthalene, fluorene is the donor and naphthalene is the acceptor. Since the two intervening methylene carbons on the naphthalene side are sp^3 hybridized, the symmetry of spirofluorenenaphthalene is different from that of spirobifluorene and spirofluorenephenanthrene. The naphthalene plane bends away from the short axis of fluorene and makes the C_{2v} axes of fluorene and dimethylnaphthalene incline at a tetrahedral angle of 109.5°. Thus, only the long molecular axis of dimethylnaphthalene is perpendicular to the $S_1 \leftarrow S_0$ transition moment of fluorene. The $S_1 \leftarrow S_0$ and $S_2 \leftarrow S_0$ transition moments in naphthalene are respectively long and short axes polarized,[16] and therefore, dipolar coupling from fluorene is forbidden to the S_1 but allowed to the S_2 state of naphthalene if the symmetry of the molecule is maintained.[20,21] Energy transfer via exchange couplings is also forbidden in the symmetric molecule because the π systems of the two rings are orthogonal.[22]

In spirofluorenenaphthalene, the S_{1N} state is at 31 325 cm^{-1}, the S_{1F} state is at 33 512 cm^{-1} (energy gap = 2187 cm^{-1}), and the S_{2N} state is probably at 33 800 cm^{-1}. Since the S_{1F} origin of spirofluorenenaphthalene lies roughly 300 cm^{-1} below the S_{2N} origin, electronic energy transfer from fluorene to dimethylnaphthalene must be vibrationally mediated for the S_{1F} origin and low-lying vibronic states but might be enhanced by direct dipolar coupling when higher vibronic levels of the donor are excited.

Table 10 gives the rate of electronic energy transfer in spirofluorenephenanthrene and spirofluorenenaphthalene at different vibronic levels inferred from the spectral broadening using eq 3. In neither molecule is there any dramatic dependence of the electronic energy transfer rate on vibronic excitation. If there is any increase in rate in spirofluorenenaphthalene above the S_{2N} origin, the effect is small. Presumably, the density of states of the S_{2N} state is low, and direct dipolar coupling with the S_{1F} state depends on accidental coincidences.[3]

TABLE 10: Rate of Electronic Energy Transfer in Spirofluorenephenanthrene (SFP) and Spirofluorenenaphthalene (SFN) at Different Vibronic Energy Levels

molecule	excess energy/cm^{-1}	Δ_{DA}/cm^{-1}	Γ^a/cm^{-1}	$k_{EET}/10^{12}$ s^{-1}
SFP	0	6.43	6.05	1.14
	+150	3.85	3.22	0.61
	+404	3.84	3.21	0.60
	+728	6.31	5.93	1.12
	+985	4.54	4.01	0.76
	+997	5.45	5.00	0.94
SFN	0	3.37	2.65	0.50
	+169	2.77	1.90	0.36
	+204	3.69	3.03	0.57
	+400	6.08	5.68	1.07
	+688	4.32	3.76	0.71
	+853	7.04	6.69	1.26
	+985	4.55	4.02	0.76

[a] $\Delta_D = 1.83$ cm^{-1} is assumed.

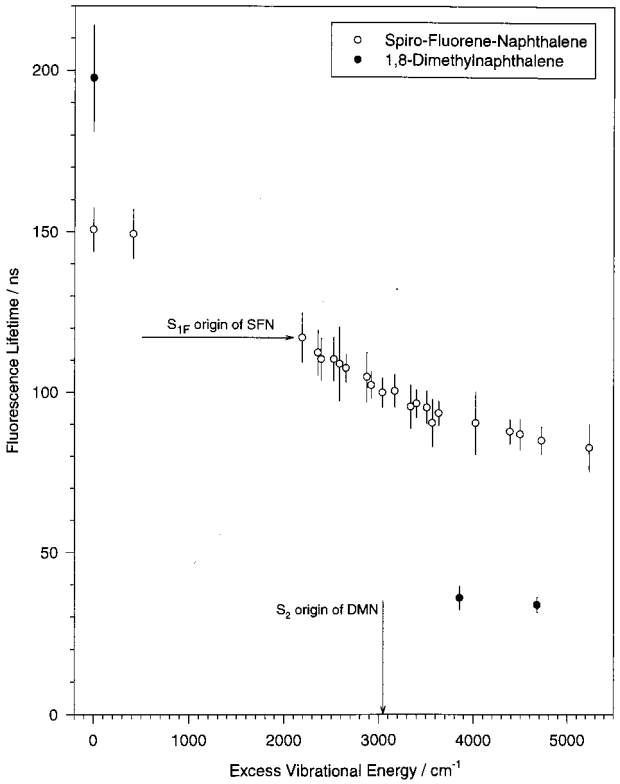

Figure 13. Fluorescence lifetime of spirofluorenenaphthalene at different excess vibrational energies above the S_{1N} origin. The three filled circles are the fluorescence lifetimes of 1,8-dimethylnaphthalene measured at the S_1 origin and two other levels above the S_2 origin.

As in the case of spirofluorenephenanthrene, electronic energy transfer in spirofluorenenaphthalene produces a lengthening of the fluorescence lifetime from that of fluorene (16.7 ± 0.8 ns) to that of dimethylnaphthalene (198 ± 16.4 ns). The variation in the lifetime of spirofluorenenaphthalene with excess vibrational energy is plotted in Figure 13. The fluorescence lifetime of spirofluorenenaphthalene at the S_{1N} origin is 151 ± 8 ns. The lifetime drops to 117 ± 8 ns at the S_{1F} origin and it keeps decreasing slowly until it levels off at even higher vibrational energy. Variations in the fluorescence lifetime have been observed in substituted naphthalenes. These variations reflect the changes in the rate of radiationless decay that leads to intersystem crossing to the low-lying T_1 state. In general, the rate of radiationless decay increases with the density of states of the T_1 state.[19] In Figure 13, we have also plotted three points for the model compound, dimethylnaphthalene. Both the magnitude and energy dependence of these lifetimes are different from those of spirofluorenenaphthalene. This is not surprising considering the different vibrational frequencies in the two molecules. The very low frequency modes associated with the nearly free internal rotation of the methyl groups in dimethylnaphthalene are shifted to much higher frequency when the methyl groups are bound to fluorene in spirofluorenenaphthalene. This would have a significant effect on the density of states and on the rate of radiationless decay.

C. 2,7-Dichlorospirobifluorene and 4,5-Diazospirobifluorene. The two remaining large energy gap spiranes, dichlorospirobifluorene and diazospirobifluorene, exhibited the same qualitative behavior as spirofluorenephenanthrene and spirofluorenenaphthalene. Specifically, in the case of dichlorospirobifluorene, only the characteristic dichlorofluorene (acceptor) emission was observed upon excitation of any vibronic transition of the donor, proving that a complete singlet excitation transfer occurred regardless of which vibrational state of the donor was initially populated.

The fluorescence of the monomeric diazofluorene was not sufficiently strong to be detected in the molecular beam experiments. From the weak emission in solution, we estimate that the S_1 state of diazofluorene is approximately 1100 cm^{-1} lower in energy than the S_1 state of fluorene. Attempts to excite bichromophoric diazospirobifluorene in the spectral region of the fluorene absorption also did not yield measurable emission in the molecular beam experiment. It was concluded that the donor fluorescence is quenched via rapid singlet excitation transfer from the S_1 state of fluorene to the nonemissive S_1 state of diazofluorene.

Conclusions

Electronic energy transfer has been observed in spirofluorenephenanthrene and spirofluorenenaphthalene. In these two molecules, emission exclusively from phenanthrene and naphthalene was observed upon exciting the fluorene origin (S_{1F}). The special symmetry of these two molecules prohibits energy transfer by either dipolar or exchange couplings if the symmetry of the molecules is maintained. The occurrence of energy transfer in spirofluorenephenanthrene and spirofluorenenaphthalene is explained by vibronic coupling via nontotally symmetric vibrations. Nontotally symmetric vibrations break the symmetry of the molecule and reactivate both dipolar and exchange couplings that promote electronic energy transfer. The observed spectral broadening indicates that the rate of energy transfer is substantially faster than the radiative decay rate of fluorene, consistent with the fact that only acceptor like emission was observed. The very large energy gap between the donor and the acceptor also suggests that radiationless relaxations in these two molecules occur in the statistical limit. Thus, electronic energy transfer is rapid and irreversible. This is in marked contrast to the behavior observed in spirobifluorene, where the rate of energy transfer strongly depends on accidental coincidences of energy levels between the donor and the acceptor.

Acknowledgment. The work in the laboratory of D.H.L. was supported by the National Science Foundation under Grant CHE-9319958. The work in the P.P. laboratory was supported by the Office of Basic Energy Sciences, U.S. Department of Energy, through Grant DE-FG02-97ER14756. The authors thank Mr. Gene A. Plaisance for his contribution to the synthesis of one of the model compounds.

References and Notes

(1) (a) Speiser, S. *Chem. Rev.* **1996**, *96*, 1953 and references therein. (b) Newton, M. D. *Chem. Rev.* **1991**, *91*, 767 and references therein. (c) Chattoraj, M.; Bal, B.; Closs, G. L.; Levy, D. H. *J. Phys. Chem.* **1991**, *95*, 9666. (d) Chattoraj, M.; Bal, B.; Shi, Y.; Closs, G. L.; Levy, D. H. *J. Phys. Chem.* **1993**, *97*, 13046. (e) Chattoraj, M.; Chung, D. D.; Bal, B.; Closs, G. L.; Levy, D. H. *J. Phys. Chem.* **1994**, *98*, 3361. (f) Closs, G. L.; Piotrowiak, P.; Miller, J. R. In *Photochemical Energy Conversion*; Norris, J., R., Jr., Meisel, D., Ed.; Elsevier: New York, 1989. (g) Maki, A. H.; Weers, J. G.; Hilinski, E. F.; Milton, S. V.; Rentzepis, P. M. *J. Chem. Phys*. **1984**, *59*, 2288.

(2) (a) Zeng, Y.; Zimmt, M. B. *J. Am. Chem. Soc*. **1991**, *113*, 5107. (b) Zeng, Y.; Zimmt, M. B. *J. Phys. Chem.* **1992**, *96*, 8395. (c) Oliver, A. M.; Paddon-Row, M. N.; Kroon, J.; Verhoeven, J. W. *Chem. Phys. Lett.* **1992**, *191*, 371. (d) Kumar, K.; Lin, Z.; Waldeck, D. H.; Zimmt, M. B. *J. Am. Chem. Soc*. **1996**, *118*, 243.

(3) van Dantzig, N. A.; Levy, D. H.; Vigo, C.; Piotrowiak, P. *J. Chem. Phys.* **1995**, *103*, 4894.

(4) No exciton splitting and no acceptor fluorescence were detected, indicating that the electronic coupling was smaller than the spectral resolution of the experiment ($\sim$0.05 cm^{-1}) and that the singlet excitation transfer, if present, was several orders of magnitude slower than the decay of the donor S_1 state, $\tau > 20$ ns.

(5) (a) Zasukha, V. A. *Chem. Phys*. **1988,** *128*, 289. (b) Glauser, W. A.; Raber, D. J.; Stevens, B. *J. Phys. Chem.* **1991**, *95*, 1976.

(6) It is a common practice in the field of excitation and electron-transfer studies to use the first-order perturbation theory methods to estimate the electronic coupling between the donor and the acceptor. In the simplest and most frequently used approach, the off-diagonal electronic matrix elements, V_{DA}, are obtained from the splittings (i.e., the shifts of the diagonal elements) calculated at the ab initio or semiempirical level for a degenerate donor−acceptor pair and transferred to the nondegenerate systems under study. A better solution involves a calculation on a realistic donor−acceptor pair and direct extraction of the off-diagonal elements. Since both approaches by default calculate the coupling between the $v = 0$ levels of the donor−acceptor pair, neither of them is capable of accounting for the presence of strong vibronic coupling. Therefore, in cases with complete symmetry cancellations of the Coulomb and exchange integrals involving the localized electronic wave functions of the donor and the acceptor, such calculations do not yield a useful estimate of the magnitude of the electronic interaction between the two chromophores.

(7) Piotrowiak, P.; Kobetic, R.; Schatz, T.; Tapper, S. *Bull. Pol. Acad. Sci.* **1994**, *42*, 445.

(8) Sharfin, W.; Johnson, K. E.; Wharton, L.; Levy, D. H. *J. Chem. Phys.* **1979**, *71*, 1292.

(9) Müller, M.; Hohlneicher, G. *J. Am. Chem. Soc.* **1990**, *112*, 1237.

(10) Healy, E. F.; Holder, A. *J. Mol. Struct.* **1993**, *281*, 141.

(11) Ohta, N.; Baba, H. *Mol. Phys.* **1986**, *59*, 921.

(12) Warren, J. A.; Hayes, J. M.; Small, G. J. *Chem. Phys.* **1986**, *102*, 323.

(13) Schettino, V.; Neto, N.; Califano, S. *J. Chem. Phys.* **1966**, *44*, 2724.

(14) Chakraborty, T.; Chowdhury, M. *Chem. Phys.* **1992**, *159*, 439.

(15) Beck, S. M.; Powers, D. E.; Hopkins, J. B.; Smalley, R. E. *J. Chem. Phys.* **1980**, *73*, 2019.

(16) Behlen, F. M.; McDonald, D. B.; Sethuraman, V.; Rice, S. A. *J. Chem. Phys.* **1981**, *75*, 5685.

(17) Warren, J. A.; Hayes, J. M.; Small, G. J. *J. Chem. Phys.* **1984**, *80*, 1786.

(18) Ichimura, T.; Auty, A. R.; Jones, A. C.; Phillips, D. *J. Spectrosc. Soc. Jpn.* **1985**, *34*, 83.

(19) Jacobson, B. A.; Guest, J. A.; Novak, F. A.; Rice, S. A. *J. Chem. Phys.* **1987**, *87*, 269.

(20) Förster, T. *Discuss. Faraday Soc.* **1959**, *27*, 7.

(21) Förster, T. *Ann. Physik.* **1948**, *2*, 55.

(22) Dexter, D. L. *J. Chem. Phys.* **1953**, *21*, 836.

(23) Bixon, M.; Jortner, J. *J. Chem. Phys.* **1968**, *48*, 715.

(24) Freed, K. F.; Jortner, J. *J. Chem. Phys.* **1969**, *50*, 2916.

(25) Freed, K. F. *J. Chem. Phys.* **1970**, *52*, 1345.

(26) Amirav, A.; Sonnenschein, M.; Jortner, J. *J. Chem. Phys.* **1984**, *88*, 5593.

(27) There is extensive literature on the evaluation of the Voight line shape (see the following: Armstrong, B. H. *J. Quant. Spectrosc. Radiat. Transfer* **1967**, 7, 61 and references contained therein. For the following formula for evaluating the Voight profile in the limit where the homogeneous line width is greater than the inhomogeneous line width, see:

$$\Gamma = [\Delta_{DA}{}^2 - [\Delta_D{}^2/(2 \ln 2)]\}/\Delta_{DA} \quad (4)$$

Amirav, A.; Sonnenschein, M.; Jortner, J. *J. Phys. Chem.* **1984**, *88*, 5593. Use of this formula gives a value of $\Gamma = 6.05$ cm^{-1}.

(28) Bree, A.; Zwarich, R. *J. Chem. Phys.* **1969**, 51, 903. (b) Bree, A.; Zwarich, R. *J. Chem. Phys.* **1969**, 51, 912.